iScience

CellPress
OPEN ACCESS

Article

Local adaptive immunity in atherosclerosis with T cell activation by aortic dendritic cells accelerates pathogenesis

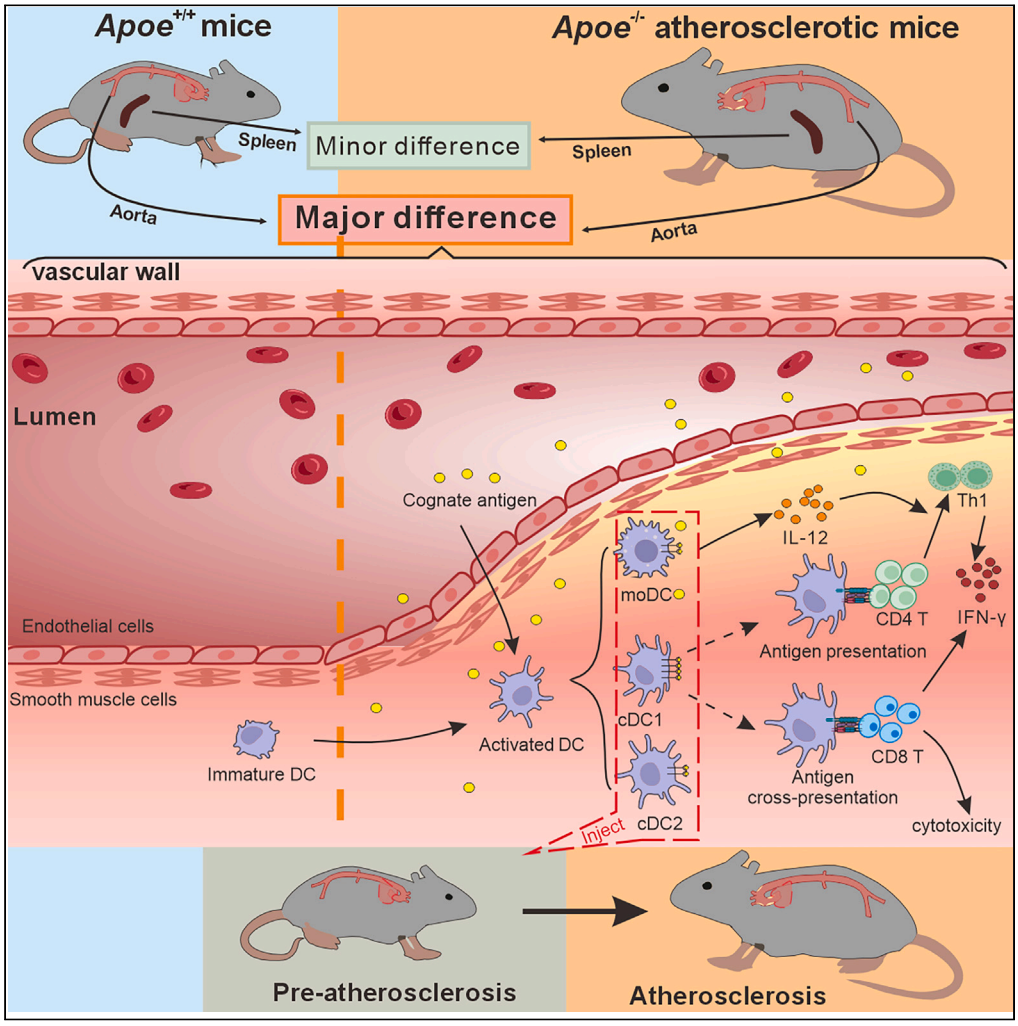

Wenjie Zhang, Zecheng Cai, Dan Ma, ..., Li Sun, Andrew M. Lew, Yuekang Xu

yuekang.xu@hotmail.com

Highlights

Atherogenesis involves the accumulation of myeloid cells and lymphocytes in the aorta, not the spleen

Atherogenesis specifically upregulates adaptive T cell immunity by DCs among aortic APCs

GM-CSF-dependent moDCs promote Th1 differentiation and cDC1 activate CD8⁺T cells in aorta

Identification of distinct roles of aortic DCs may offer targeted therapy in diseased loci

Zhang et al., iScience 27, 111144
November 15, 2024
https://doi.org/10.1016/j.isci.2024.111144

iScience

CellPress
OPEN ACCESS

Article

Local adaptive immunity in atherosclerosis with T cell activation by aortic dendritic cells accelerates pathogenesis

Wenjie Zhang,[1] Zecheng Cai,[1] Dan Ma,[1] Meng Liu,[1] Juncheng Wang,[1] Li Sun,[1] Andrew M. Lew,[2] and Yuekang Xu[1,3,*]

SUMMARY

Atherosclerosis represents a chronic inflammatory condition in arterial walls, where local immune cells significantly contribute to disease progression. This study employed various *in situ* immunological techniques to investigate the specific roles of aortic dendritic cell (DC) subsets in atherosclerotic animal models, distinguishing between normal and diseased immune contexts. Our findings revealed that aortic DCs, particularly the cDC1 subset, played a critical role in facilitating $CD8^+$ T cell activation through antigen presentation. Additionally, atherosclerosis-induced increases in GM-CSF levels enhanced CCR7 expression on aortic monocyte-derived DCs, promoting their recruitment and IL-12 production for Th1 differentiation. Notably, immunizing pre-atherosclerotic mice with DC-presented antigens or transferring aortic DCs from atherosclerotic mice resulted in accelerated disease onset. This research elucidates the adaptive immune functions of aortic DCs, offering insights into the cellular mechanisms driving aortic inflammation and potential therapeutic targets for atherosclerosis management.

INTRODUCTION

Atherosclerosis is a root cause of many serious cardiovascular diseases such as coronary heart disease and stroke, characterized by the formation of lipid plaques, and inflammation in medium or large arteries with circulating autoantibodies, where both innate and adaptive immunity play important roles.[1,2] Adaptive immunity mediated by T cells is a key modulator of atherosclerosis,[3,4] as highly activated phenotypes of auto-reactive T cells have been identified in atherosclerotic plaques.[5,6] For $CD4^+$ T helper (Th) cells, Th1 cells promoted lesion development,[7–9] whereas regulatory T cells (Tregs) correlated negatively with atherogenesis.[10,11] Th2 and Th17 cells in plaques were also found to be associated with the development of atherosclerosis, although their roles in atherosclerosis remain controversial.[10,12–16] In addition, both pro- and anti-atherogenic effects of $CD8^+$T cells through either cytotoxic activity against lesion-stabilizing cells or the production of inflammatory cytokines have been reported.[17]

Dendritic cells (DCs) are regarded as professional antigen-presenting cells (APCs), being able to present to naive T cells. They have been found in both human and mouse blood vessels and are thought to be associated with the formation of foam cells and lipid metabolism during atherogenesis.[18,19] With the recent finding of the importance of $CD40^-$CD40L interaction between DCs and T cells in the development of disease,[20] several studies have suggested that DCs may play a key role in activating auto-reactive T cells in the aorta.[21,22] Unfortunately, these studies mainly considered systemic DCs,[21–24] leaving open the contribution of aortic DCs. We opined that aortic DCs by the nature of their proximal location were likely to be intimately involved and may play a role at every stage of disease progression. Furthermore, the results of those studies were mostly derived from gene-knockout animals, whereby deficiency of one protein or cell type from embryo to adulthood might lead to the compensation of other molecules or cell lineages, masking the original contribution of targeted cells under native conditions. Therefore, the adaptive roles of the most powerful antigen-presenting cells (APCs) in the diseased locus are still obscure, let alone their differential roles at subset levels.

Indeed, using advanced single cell techniques, recent studies have found that aortic DCs comprise heterogeneous subsets.[25,26] However, the division of labor among these DC subsets in the aorta during atherogenesis was not further pursued. Although some studies based on genetically modified mice have shed interesting light on the role of some DC subsets in atherosclerosis, the conclusions of different studies have often been contradictory.[27] For example, Flt3-dependent $CD103^+$DCs have been reported to inhibit plaque development by modulating Tregs and IL-10 levels in $LDLR^{-/-}$ mice.[24] However, others have found that the deletion of Batf3-dependent $CD103^+$DCs did not affect

[1]Anhui Provincial Key Laboratory for Conservation and Exploitation of Biological Resources, College of Life Sciences, Anhui Normal University, Wuhu 241000, China
[2]The Walter and Eliza Hall Institute of Medical Research, University of Melbourne, Parkville, VIC, Australia
[3]Lead contact
*Correspondence: yuekang.xu@hotmail.com
https://doi.org/10.1016/j.isci.2024.111144

atherosclerotic lesion formation in mice,[28] or even report a pro-atherogenic role for CD103$^+$DCs in other models.[29] These conflicting results could be caused by either different model specific pathologies or the absence and compensation of different molecules in the development of atherosclerosis.

To understand the authentic roles of regional DCs during autoinflammatory atherogenesis in animals with a native immune system, we classified aortic DCs for the first time into complete subsets and made real-time investigations into the dynamic changes in proinflammatory parameters across the disease-associated tissues *in situ* before and after atherosclerosis and have identified the adaptive roles of aortic DCs at subset levels in the development of atherosclerosis.

RESULTS

Dendritic cell numbers increase significantly in the aorta during atherogenesis

The gating strategy used in this study to define immune cells in the aorta (as non-lymphoid tissues) was adopted from published studies,[30–33] with slight modifications. After debris and cell doublets were eliminated by FSC-A vs. SSC-A and FSC-H vs. FSC-A, total live leukocytes were collected based on the exclusion of dead cells by their PI$^+$ staining. Leukocytes were analyzed based on their expression of CD45 (R1). Neutrophils were distinguished from all other leukocytes (R2) based on their expression of Ly6G (Figure 1A). The myeloid leukocytes (R3), after excluding CD11c$^-$CD11b$^-$ population (R4), were first subdivided based on their pattern of SSC-A vs. MHC-II expression. As reported,[30] the MHC-II$^-$SCC^{lo} population (R5) contained NK cells and monocytes, which could be distinguished based on their expression of CD11b and CD64: monocytes are CD11b^{hi}CD64^{int}, and NK cells are CD11b^{int}CD64$^-$ that were also identified by NK1.1(Figure S1A). Then within R6 in the MHC-II/SSC staining, F4/80$^+$MerTK$^+$ macrophages (Mϕ) and subsequently CD11c^{hi}MHC-II^{hi}DCs were finally identified (Figure 1A). Furthermore, within the DC gate, we went on to examine their subsets, which included CD11c$^+$MHCII$^+$CD64$^+$ moDCs, CD11c$^+$MHCII$^+$B220$^+$ pDCs, CD11c$^+$MHCII$^+$CD11b$^+$XCR1$^-$ cDC2s and CD11c$^+$MHCII$^+$XCR1$^+$CD11b$^-$ cDC1s (Figure 1B). In addition, from the CD11c$^-$CD11b$^-$ region (R4) we defined B220$^+$MHC-II$^+$ B cells, and CD3$^+$ T cells in the remaining B220$^-$MHC-II$^-$ gate (Figure 1C).

To identify the immune cell type(s) responsible for the inflammatory disease, we first compared the disease-associated dynamic changes of the immune cell components identified above between healthy and AS mice in both disease target tissue (vascular tissues) and classical lymphoid organ (spleens). We calculated the number of cells per milligram of tissues processed to determine the changes in immune cell populations in the disease-altered tissues. We found that the number of leukocytes in the atherosclerotic aorta was significantly higher, in which the number of both myeloid cells such as neutrophils, DCs, and Mϕ, and lymphocytes such as T and B cells (Figure S1B) were increased in the atherosclerotic aorta. During disease, DC numbers increased approximately 5-fold, which was the most dramatic of any cell type (Figure 1D). Interestingly, this increase was mainly due to moDCs, whereas no significant increases were observed in other subsets (Figure 1E). Deep analysis of the factors that resulted in the most increased moDCs demonstrated an enhanced level of granulocyte macrophage colony stimulating factor (GM-CSF), a key growth factor for moDCs, specifically in the vascular tissues, rather than the spleens, of the atherosclerotic mice (Figure 1F). Concordantly, the proportion of moDCs was significantly increased in the wild-type aorta of mice inoculated with GM-CSF-expressing B16 melanoma cells (B16-GM), while other DC subsets were unchanged or decreased (Figure 1G). Further mechanistic exploration of the specific increase of moDC subset revealed the upregulation of CCR7 on their surface in response to GM-CSF from B16 cells (Figure 1H). To deeply investigate the primary cell types responsible for GM-CSF production in the atherosclerotic aorta, we found that, compared to normal aortas, neutrophils, Mϕ, and CD45$^-$non-immune cells in atherosclerotic aortas exhibited substantially elevated GM-CSF expression levels (Figure S1F).

In contrast, in the spleen of the same mice, the changes in the composition of immune cells during atherogenesis were less remarkable. Although extramedullary hematopoiesis characterized by slightly enhanced leukocyte numbers including neutrophils and DCs in atherosclerosis was observed, other immune cells showed little change (Figures S1C and S1D). In particular, the number of various DC subsets in the spleen was not significantly different between normal and atherosclerotic mice (Figure S1E). Collectively, we observed that during the development of atherosclerosis, the dynamic changes of immune cells and their molecular mediators occurred in the local diseased region aorta, the most dramatic of which was DCs, indicating potential pathological roles for these APCs.

Enhanced effector:naive ratio of aortic CD8$^+$T cells correlates with activated antigen-presenting cells, especially dendritic cells, in the atherosclerotic aorta rather than spleen

Next, we explored the activation status of aortic T cells. Consistent with previous reports,[34] CD4$^+$ T cells in the aortic walls of atherosclerotic mice demonstrated activated phenotypes in terms of CD69 expression and BrdU incorporation (Figures S2A and S2B). In addition, we found that aortic CD8$^+$T cells also upregulated CD69 (Figure 2A), and there was an increased proportion of proliferated Ki67$^+$ CD8$^+$T cells *in situ* after atherosclerosis (Figure 2B); this was confirmed by BrdU uptake *in vivo* (Figure 2C). Moreover, CD8$^+$T cells were also found to secrete more IFNγ (Figure 2D) in response to the onset of the disease, consistent with an autoimmune destructive process. Most importantly, we found that the CD8$^+$T cells in atherosclerotic aorta demonstrated an increased proportion of CD44$^+$CD62L$^-$effector memory T cells (T_{EM}), while that of CD44$^-$CD62L$^+$ naive T cells (Figure 2E) were reduced when the mice developed atherosclerosis from a non-atherosclerotic state. This is similar to what we and others have found for CD4$^+$ T cells in atherosclerotic aorta (Figure S2C).[6,34] These findings are consistent with the possibility that naive T cells become activated *in situ*. In the spleens of the same mice, however, we found that although the effector:naive ratio of CD8$^+$ T and CD4$^+$ T cells increased (Figures 2F and S2D) in response to atherogenesis, CD69 and Ki67 expressed by CD8$^+$ (Figures 2G and

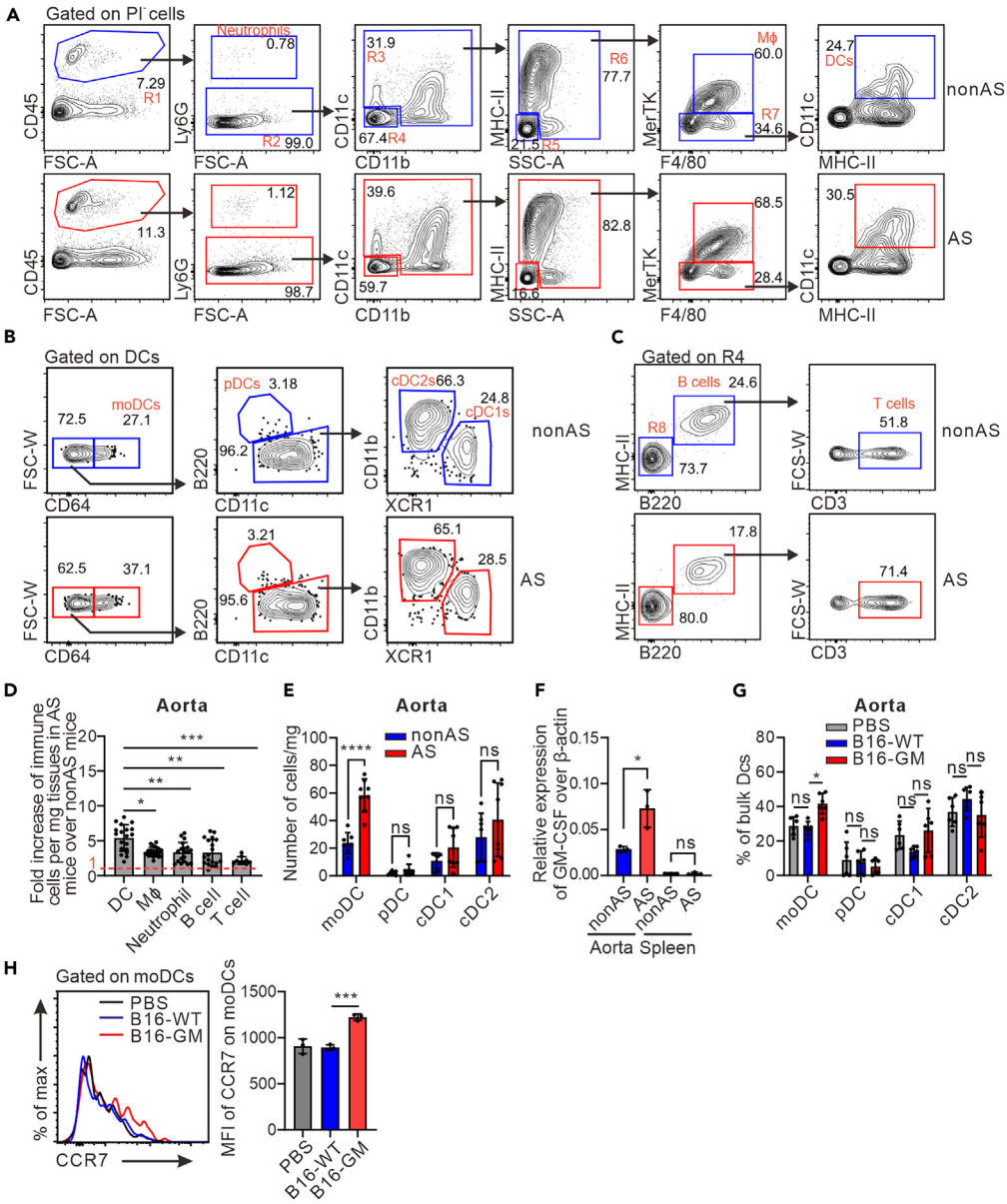

Figure 1. DC numbers increase significantly in the aorta during atherogenesis

Single cell suspensions from aortas or spleens were stained with indicated antibodies for FACS or used in RT-qPCR. Gates containing multiple cell populations are numbered (R1-R8), whereas the gates containing a single cell population are labeled with the included cell type (A–C). Bar graphs showed the fold changes of different immune cells per mg tissues in atherosclerotic aorta (n = 9–19) (D); the number of DC subsets per mg tissues in aorta (n = 7–8) (E); the relative expression of GM-CSF in aorta and spleens (n = 3) (F); the proportion of various DC subsets in the aorta of C57BL/6 mice injected with PBS, B16-WT or B16-GM (n = 3) (G). Single cell suspensions from aortas were prepared for FACS analysis. Plots and bar graphs showed the proportion of GM-CSF (n = 5–6) (H). All data were shown as Mean ± SD, and the one-way ANOVA test or Kruskal-Wallis test was used in (D, G, and H), two-tailed unpaired t test, and two-tailed Mann Whitney test was used in (E, F). *$p < 0.05$, **$p < 0.01$, ***$p < 0.001$ ****$p < 0.0001$. ns, no significant difference; nonAS, *Apoe*$^{+/+}$ mice under high-fat diet; AS, *Apoe*$^{-/-}$ atherosclerotic mice under high-fat diet; B16-WT, B16 wild-type mouse melanoma cells; B16-GM, B16-WT expressing GM-CSF.

2H) or CD4$^+$T cells (Figures S2E and S2F) was little changed from non-arherosclerotic mice. Likewise, the expression of IFNγ (Figure 2I) in CD8$^+$T cells from atherosclerotic spleens was comparable to that of normal mice.

Concordant with the heightened numbers of activated T cells in the atherosclerotic aorta, we further identified significant upregulation of the co-stimulatory molecule CD80, CD86 and CD40 on potential APCs, such as DCs, Mϕ, and B cells in the atherosclerotic aorta (Figures S2G, S2H, and 2J), but not in the spleen (Figures S2G, S2H, and Figure 2K). Interestingly, CD40 upregulation was most prominent in DCs (>2-fold) (Figure 2J).

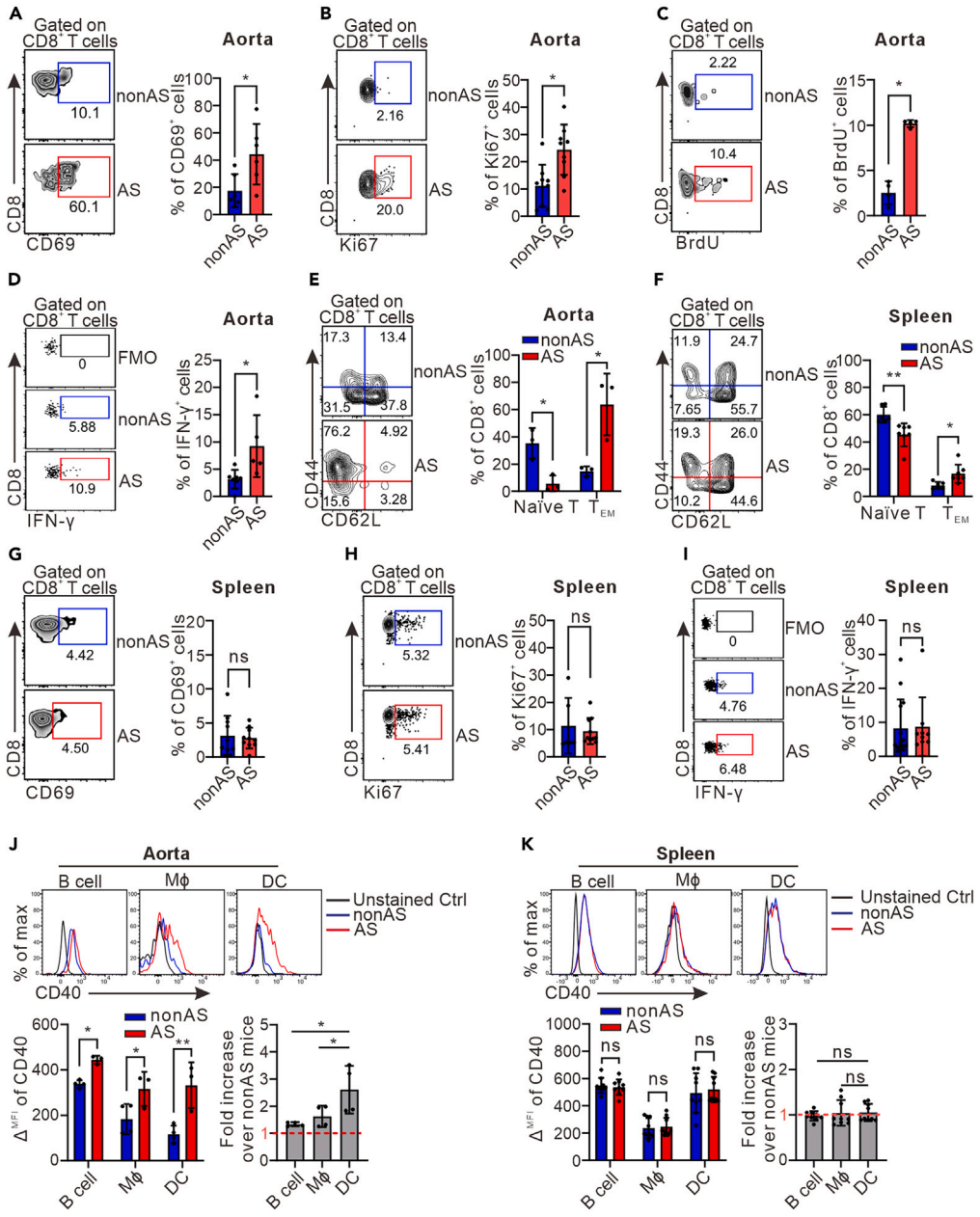

Figure 2. Enhanced effector/naive ratio of aortic CD8$^+$ T cells correlates with activated APCs in the aorta

Single cell suspensions from aortas or spleens were prepared and gated on CD8$^+$ T cells for FACS analysis. Plots and bar graphs showed the percentage of CD69 expression in the aorta (n = 6) (A) or spleen (n = 10) (G); Ki67 expression in aorta (n = 9) (B) or spleen (n = 6–10) (H); BrdU expression in aorta after *i.p.* injection for 1h (n = 4) (C); IFNγ expression in aorta (n = 5–7) (D) or spleen (n = 9–14) (I); CD62L$^+$CD44$^-$ naive T cells and CD62L$^-$CD44$^+$ T_{EM} cells in aorta (n = 3) (E) or spleen (n = 6–7) (F). Alternatively, the expression of CD40 on B cells, Mϕ, and DCs, as well as their fold increase from the single cell suspensions in AS vs. non-AS mice in the aorta (n = 4) (J) or spleens (n = 9) (K) were also analyzed. All data were shown as mean ± SD and analyzed using a two-tailed unpaired t test, two-tailed Mann-Whitney test, or one-way ANOVA test. *$p < 0.05$, **$p < 0.01$, ***$p < 0.001$. ns, no significant difference.

Only aortic DCs, especially the cDC1 subset, affect antigen presentation during atherogenesis

To further identify which APCs induced the observed T cell activation in the atherosclerotic tissues, we compared DCs, Mϕ, and B cells for their capacity to present model antigen OVA both *in vitro* and *in vivo* during atherogenesis. In *Apoe*$^{+/+}$ mice under a high-fat diet, only DCs could present OVA antigen *in vitro* to stimulate OVA-specific OT-II CD4$^+$ T cell proliferation in both aortic and splenic tissues among all the APCs (Figures 3A and S3A). Interestingly, when the mice developed atherosclerosis, this unique CD4$^+$ T cell-stimulating capacity could be further enhanced, whereas other APCs still remained incompetent (Figures 3A and S3A). Furthermore, only aortic DCs showed elevated expression of

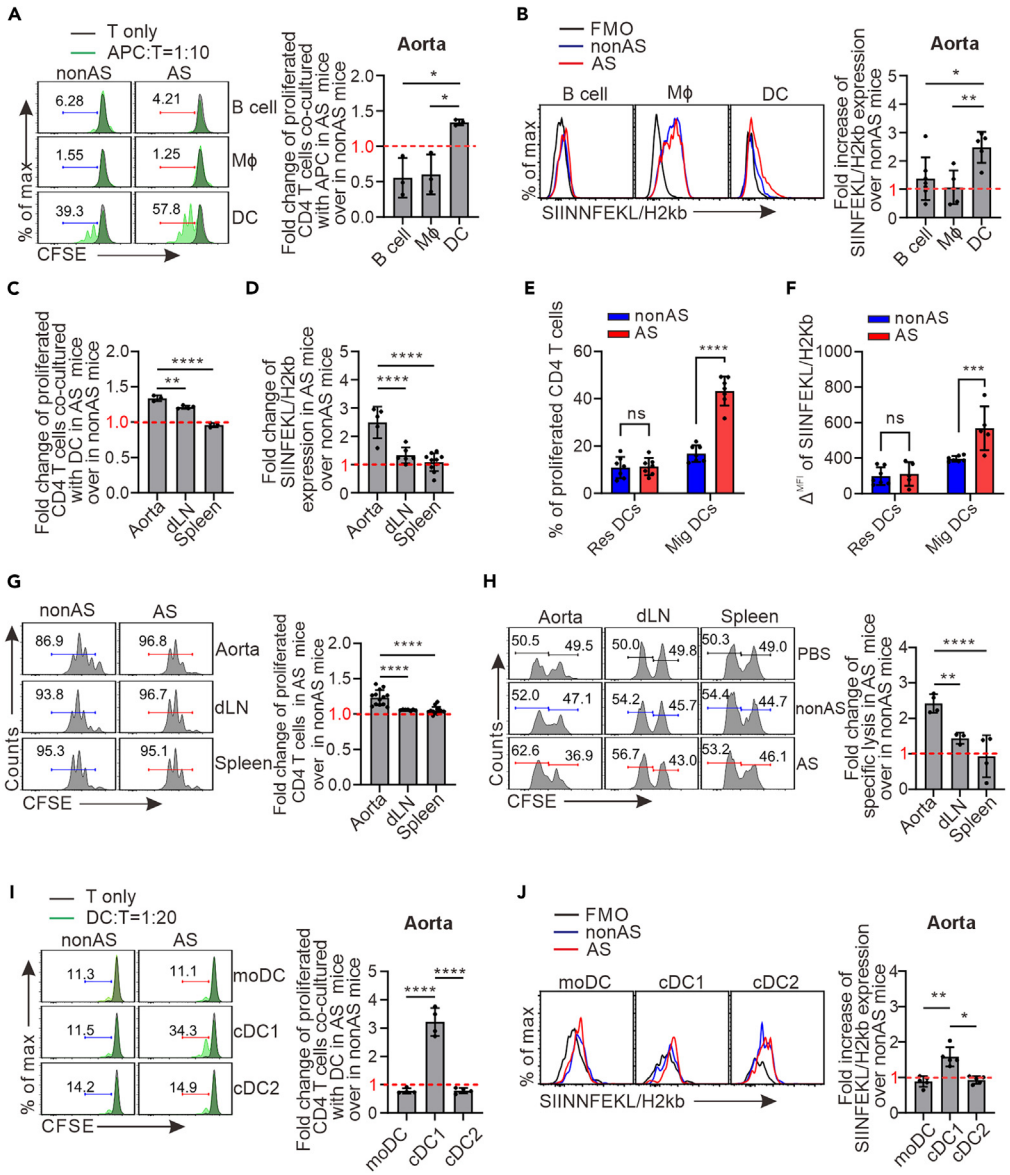

Figure 3. DCs, especially the cDC1 subset, affect antigen presentation during atherogenesis

Sorted B cells, Mϕ, and DCs from aortas, draining LNs or spleens were co-cultured with OT-II CD4$^+$T cells in the presence of OVA for 3 days before the proliferation of CD4$^+$T cells were measured *in vitro* (n = 3–4) (A–C). Mice were *i.v.* injected with 1.5mg OVA for 24h before the expression of SIINFEKL/H2kb on APCs from aortas, draining LNs, and spleens were examined *ex vivo* (n = 5–10) (B–D). Migratory and resident DCs in aortic draining LN were sorted for similar experiments as in (A) or (B), and the bar graph show the proportion of proliferated OT-II CD4$^+$ T cells (*n* = 7) (E) or the expression of SIINFEKL/H2Kb on different DC population in aortic draining LNs (n = 5–7) (F) respectively. Purified CD4$^+$ T cells from OT-II mice were labeled with CFSE and injected into mice immunized with OVA for FACS analysis of proliferated CD4$^+$ T cells *in vivo* (n = 7–13) (G). The lysis of CFSE^{high} and CSFE^{low} target cells differentially labeled with high and low concentrations of CFSE respectively as described in material and methods were examined by FACS for cytotoxic analysis in aortas, draining LNs and spleens *in vivo* (n = 3–4) (H). Cells were treated as in (A) or (B), and the proliferated CD4$^+$ T cells co-cultured with aortic moDCs, cDC1s and cDC2s (*n* = 4) (I), or the fold increase of SIINFEKL/H2kb expression on aortic moDCs, cDC1s and cDC2s (*n* = 4) (J) from AS vs. nonAS mice were shown. All data were shown as Mean ± SD and analyzed using a two-tailed unpaired *t* test or one-way ANOVA test. *$p < 0.05$, **$p < 0.01$, ***$p < 0.001$, ****$p < 0.0001$. APC, Antigen-presenting cell; FMO, Fluorescence Minus One.

surface H2Kb/SIINFEKL complexes, which reflects the ability to cross-present to CD8$^+$ T cells; this was neither observed for aortic Mϕ and B cells nor splenic DCs, Mϕ, and B cells from the same mice (Figures 3B and S3B). Anatomically, these aortic DCs with enhanced cross-antigen-presenting capacity were mainly concentrated in the aortic intima rather than the adventitia (Figure S3C). Since DCs in the draining LNs of aortic tissues may also play an important role in the activated T cells in the atherosclerotic aorta,[35] DCs isolated from the aortic draining

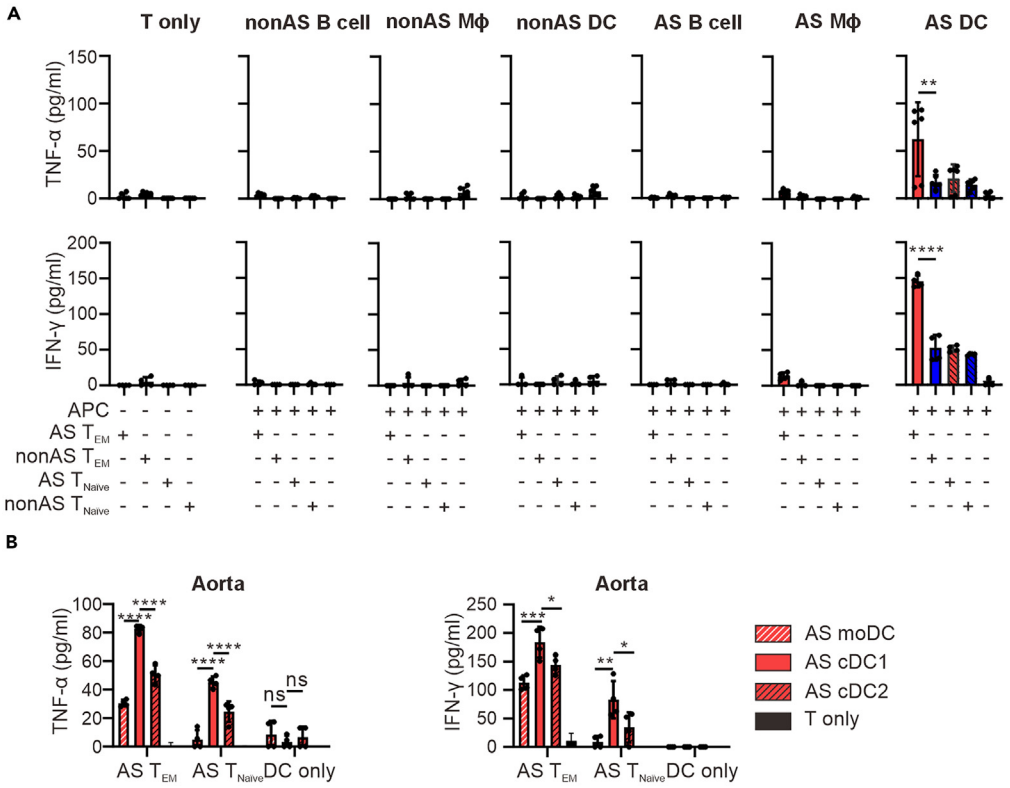

Figure 4. Enhanced cognate antigen-specific T cell stimulation in the aorta by DCs is evident during atherogenesis

(A) Sorted B cells, Mϕ, and DCs from the aorta were co-cultured with sorted $CD4^+$ naive T cells or $CD4^+$ T_{EM} cells from draining LNs for 12h before their supernatants were harvested. IFNγ ($n = 6$) and TNFα ($n = 4$) from supernatants were detected by ELISA.

(B) Sorted moDCs, cDC1s, and cDC2s from the aorta of AS mice were co-cultured with sorted $CD4^+$ naive T cells or $CD4^+$ T_{EM} cells as in (A), before IFNγ and TNFα from supernatants were detected by ELISA ($n = 4$). All data were shown as Mean ± SD and analyzed using a one-way ANOVA test. *$p < 0.05$, **$p < 0.01$, ***$p < 0.001$, ****$p < 0.0001$. ns, no significant difference.

LNs were also included for the comparison, and found that although the disease onset could indeed lead to significant upregulation of their stimulating capacity for both $CD4^+$ and $CD8^+$ T cells (Figures S3D and S3E), the fold changes were less than that of aortic DCs (Figures 3C and 3D). Interestingly, further analysis of the draining LNs classified as $CD11c^{high}$MHC-II^{low} resident DCs and $CD11c^{low}$MHC-II^{high} migratory DCs (Figure S3F), revealed that it is the migratory DCs (presumably originating from the aorta), rather than resident DCs, that exhibited the enhanced T cell stimulation after atherosclerosis *in vitro* (Figures 3E and 3F). Consistently, similar results were obtained *in vivo*, where the disease-induced proliferation of $CD4^+$ T cells (Figure 3G), and specific lysis of immunized antigen-coated $CSFE^{high}$ target cells by $CD8^+$T cells (Figure 3H) were the strongest in aorta among the three tissues, indicating the disease-targeted functional enhancement of aortic DCs.

Next, we proceeded to explore which aortic DC subset was affecting the T cell stimulation. By the same methods, we identified that cDC1s were the major DC subset both in eliciting $CD4^+$ T cell proliferation and in expressing surface H2Kb/SIINFEKL complexes (representing presentation to $CD4^+$ and $CD8^+$ T cells respectively (Figures 3I and 3J).

Since the atherosclerosis mouse model was induced in *Apoe*$^{-/-}$ mice, to rule out the impact of *Apoe* absence on DC function, we have compared the expression of co-stimulatory molecules and T cell stimulation capacity of DCs from young *Apoe*$^{-/-}$ mice without atherosclerosis to those from age-matched *Apoe*$^{+/+}$ mice, and found they were not significantly different (Figures S3G and S3H). Collectively, our findings that among APCs in the aorta, draining LNs and spleens, atherogenesis remarkably upregulated the intrinsic capacity of aortic DCs, especially the cDC1 subset, to affect T cell activation. This cogently suggested that such DCs promote the proinflammatory T cell immunity in the atherosclerotic aorta.

Enhanced cognate antigen-specific T cell stimulation by aortic dendritic cells especially cDC1 is evident in atherosclerotic aorta

To confirm whether the above findings measured with artificial model antigen really occur in the atherosclerotic diseased setting in the presence of unknown native antigens, we incubated purified $CD44^+CD62L^-CD4^+T_{EM}$ or $CD44^-CD62L^+CD4^+$ naive T cells with each cognate antigen-presented APCs if any, sorted from healthy or atherosclerotic aorta without the addition of any exogenous antigens, and quantified cytokine production from the cultured $CD4^+$T cells *in vitro* as the readout of their antigen-dependent activation. We found

that aortic APCs from non-atherosclerotic *Apoe*$^{+/+}$ mice under high-fat diets failed to induce either T_{EM} or naive T cells to secrete TNFα or IFNγ (Figure 4A). In contrast, when such mice developed atherosclerosis, DCs (but only aortic ones) could effectively induce substantial TNFα and IFNγ production from T_{EM}, whereas B cells and Mϕ in the same mice could not (Figure 4A). As expected from our findings with OVA above, splenic APCs regardless of cell type, could activate neither aortic naive T nor T_{EM} cells from either healthy or atherosclerotic mice to secrete the proinflammatory cytokines (Figures S4A and S4B). Therefore, the disease-enhanced T cell activating capacity of aortic DCs in the presence of native antigens suggests that they are the most likely APCs to stimulate local T cells during atherogenesis.

To further identify which subset of the aortic DCs account for the disease-associated T cell activation, moDCs, cDC1s, and cDC2s from the aorta in atherosclerotic mice were sorted, and co-cultured with T cells as above *in vitro*. We found that all three subsets of aortic DCs could induce TNFα and IFNγ production from T_{EM} cells but the aortic cDC1s were again the most powerful ones (Figure 4B). These results indicate that local DCs drive the activation of T cells in the atherosclerotic aorta.

Atherosclerotic aorta demonstrates a unique profile of proinflammatory T cell differentiation, in which Th1 is mostly driven by aortic moDCs

One of the important pathogenic features of atherosclerosis is the existence of proinflammatory effector T cells in the affected aortic tissues following their antigen specific activation. Consistent with previous reports on individual Th cells,[12,16,34,36] we detected an elevated proportion of IFNγ$^+$Th1 and IL-17$^+$Th17 cells, no change in IL-4$^+$Th2 cells, but reduced CD25$^+$Foxp3$^+$Tregs and IL-10-producing CD4$^+$T cells in aortic tissues when mice developed atherosclerosis in comparison with their healthy littermates (Figures S5A–S5C). In the spleen, however, there were no significant changes in Th1-, Th2-, or IL-10-producing T cells, and only slight elevations in Th17 and Tregs (Figures S5D–S5F). Therefore, these data suggest a pattern of proinflammatory T cell differentiation in the aorta with upregulated Th1/Th17, unchanged Th2, but down-regulated Treg, when mice developed atherosclerosis.

Next, we investigated the cellular sources for the local production of IL-6 and IL-12, the T cell polarization factors of the Th17 and Th1 cells respectively, in response to the onset of atherosclerosis. Increases in IL-6 production were found in a wide variety of aortic cells (neutrophils, DCs, and monocytes/NK cells; Figure 5A). In contrast, IL-12 upregulation was only found in local DCs (Figure 5B). Next we tried to determine which DC subset was producing the IL-12. We found that although all subsets can secrete IL-12 to various degrees in the healthy aorta, only moDCs significantly upregulated IL-12 production upon the development of atherosclerosis (Figure 5C); this may be particularly important given the abundance of moDCs in the atherosclerotic aorta.

Pathogenic aortic dendritic cells induce early onset of atherosclerotic plaques and atherosclerosis-like vascular inflammation in pre-atherosclerotic mice

Repeated immunization of a foreign protein to be presented by APCs *in vivo* will clonally select and expand T cells specific to that protein. OVA antigen has been demonstrated in our system to have significantly elevated presentation by aortic DCs (Figures 3A and 3B), but not splenic DCs (Figures S3A and S3B), following the development of atherosclerosis. To confirm the causal effect of aortic DCs in atherogenesis, we opined that immunizing hyperlipidemic pre-atherosclerotic *Apoe*$^{-/-}$ mice with OVA could hasten the early onset of atherosclerosis. We found that after 10 weeks on the high-fat diet, as expected, the saline-injected pre-atherosclerotic mice had not yet shown obvious lesions. In contrast, the OVA-injected mice developed prominent atherosclerotic plaques at their aortic roots (Figure 6A), as well as in the aortic arch (Figure 6B). When the control mice eventually developed atherosclerosis on a high-fat diet 14 weeks later, the area of plaque was larger in the OVA-injected mice than in the saline-injected mice at both the aortic root and the aortic arch (Figures 6A and 6B). Furthermore, immunohistology and flow cytometry analysis of the mouse aorta showed a significant increase in CD11c$^+$ DCs in OVA-injected mice (Figures 6C and S6A), and these aortic CD11c$^+$ DCs present OVA peptide SIINFEKLL on their MHCI molecules after OVA sensitization (Figure S6B). To exclude any generic vascular inflammation induced by any exogenous proteins in our system, we also immunized the pre-atherosclerotic mice with maltose-binding protein (MBP) that could not be properly presented by DCs, as the MBP-pulsed DCs were not effective in re-activating T cells for IFN-γ production in the MBP-immunized mice while OVA-pulsed DCs were in the OVA-immunized mice (Figures S6C and S6D). As expected, MBP failed to induce early onset of atherosclerosis at the time when OVA did (Figure 6D). Consistently, the proportion of Ki67$^+$CD4$^+$T cells and Ki67$^+$CD8$^+$T cells were elevated in the aorta in the OVA- but not MBP-injected mice (Figure 6E). Moreover, the aortic CD8$^+$ T cells expressed more IFN-γ only in OVA-injected mice (Figure 6F). Of note, we found that the OVA- but not MBP-injected *Apoe*$^{-/-}$ mice had also demonstrated the unique atherosclerotic inflammatory signs, with more IFNγ$^+$ Th1 and IL-17$^+$ Th17, no change in IL-4$^+$Th2 cells, and less Foxp3$^+$CD25$^+$Tregs in the aorta (Figures 6G and 6H). Furthermore, the examination of IL-12 production from the aorta showed that only DCs in OVA-injected mice expressed an increased IL-12 content (Figure S6E). Collectively, these immunological disorders induced by OVA were reminiscent of the inflammatory signatures previously identified in atherosclerosis.

The above artificial system only demonstrated that aortic DCs can be atherogenic. However, OVA is an artificial antigen, not natively expressed by atherosclerotic plaque cells. To directly validate the proatherogenic role of aortic DCs in the diseased setting, we adoptively transferred aortic DCs or splenic DCs (presumably presenting native antigen) from atherosclerotic *Apoe*$^{-/-}$ mice, or aortic DCs from non-atherosclerotic *Apoe*$^{+/+}$ mice, to young *Apoe*$^{-/-}$ mice that had not yet developed atherosclerosis under a high-fat diet, following the confirmation that the transferred DCs successfully migrated to aortic tissues (Figure S6F). Interestingly, we found that passive transfer of aortic DCs from atherosclerotic mice (but not splenic DCs from the same mice or aortic DCs from non-atherosclerotic mice) could hasten the development of atherosclerotic plaques at their aortic roots (Figure 6I). Furthermore, this pathogenic role of the transferred aortic DCs seems to rely on the

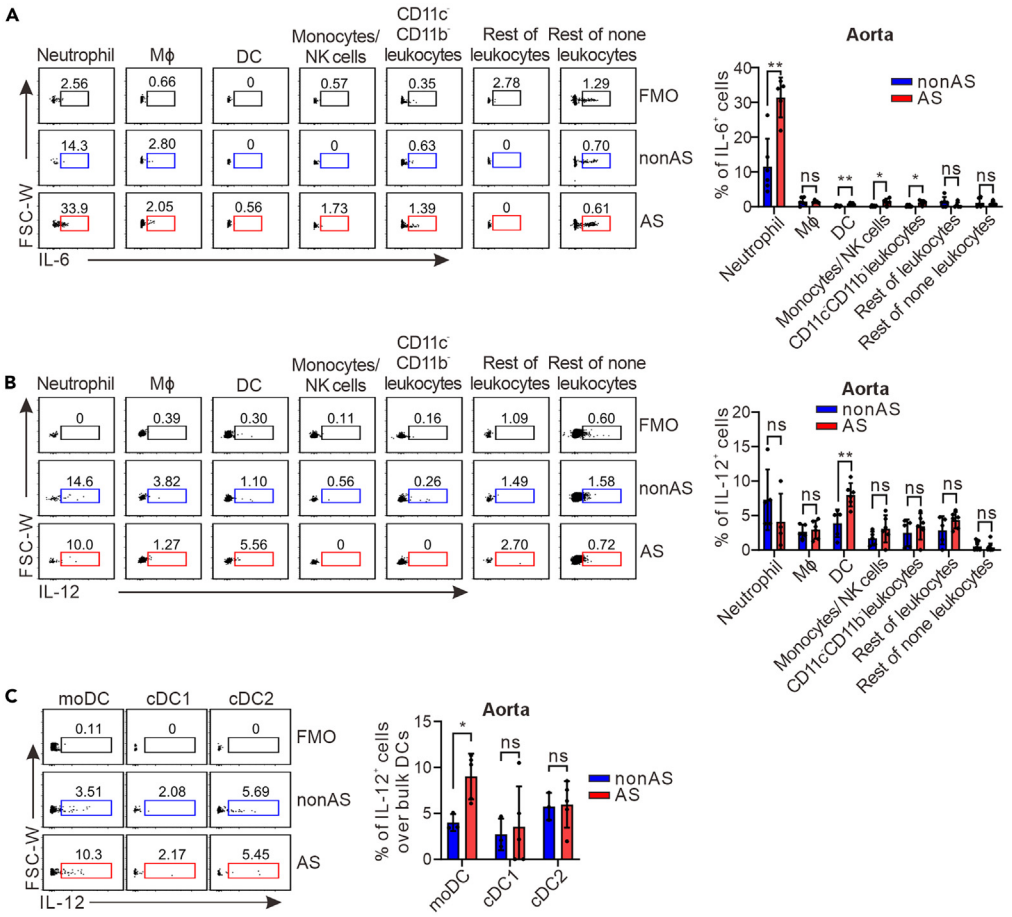

Figure 5. Atherosclerotic aorta demonstrates a unique profile of proinflammatory T cell differentiation, in which Th1 is mostly driven by aortic moDCs

Single cell suspensions from aorta were prepared for FACS analysis. Plots and bar graphs showed the proportion of IL-6- (n = 5–6) (A) or IL-12-(n = 4–6) (B) secreting cells in aorta; as well as in DC subsets (n = 3–5) (C). Individual data points represent two mice in one sample of the experiment. All data were shown as Mean ± SD and analyzed using a two-tailed unpaired *t* test or two-tailed Mann-Whitney test. *$p < 0.05$, **$p < 0.01$. ns, no significant difference; FMO, Fluorescence Minus One.

donor's diseased vascular environment, as aortic DCs from non-atherosclerotic *Apoe*$^{+/+}$ mice failed to induce the early onset of the plaques (Figure 6I).

DISCUSSION

In this study, the local immunological roles of aortic DCs in atherosclerosis-associated adaptive T cell immunity were investigated *in situ* in the presence of conventional immune components. We found that the atherogenesis is closely associated with local adaptive T cell immunity in the aorta rather than systemic spleens with local effect:naive T cell ratio increased. We identified aortic DCs as the major APCs, in contrast to Mϕ and B cells, to present aortic antigen(s) to activate local CD8$^+$, as well as CD4$^+$ T cells in atherosclerosis. The number of aortic DCs increased the most in response to the disease development, in which moDCs outnumbered other subsets due to the increased GM-CSF levels in local tissues for Th1 differentiation. There also was a division of labor amongst the DC subsets. For example, cDC1s were the most efficient at stimulating CD4$^+$ T cell proliferation and cross-presenting to CD8$^+$ T cells. Although all aortic DC subsets could produce the Th1-inducing cytokine IL-12 during atherosclerosis, moDCs were the most efficient and hence may be the most important in differentiating CD4$^+$ T cells into Th1 effectors. Finally, the aortic DC-mediated atherogenic roles were confirmed *in vivo* via the induction of atherosclerosis-like aortic inflammation and accelerating the onset of disease by DC-presented antigen and adoptive transfer of DCs from diseased aorta in the pre-atherosclerotic mice with lipid metabolic disorders. To the best of our knowledge, our data provided direct evidence, for the first time, for the pathogenic roles of comprehensive aortic DC subsets in stimulating regional adaptive T cell immunity in real time without the deletion of any immune cell type.

Although the role of DCs in mouse atherosclerosis has been well studied, our current study focused on local DCs and local aortic immunity. We were able to demonstrate several disease-associated unique changes by studying target tissues and distant tissues before and after the

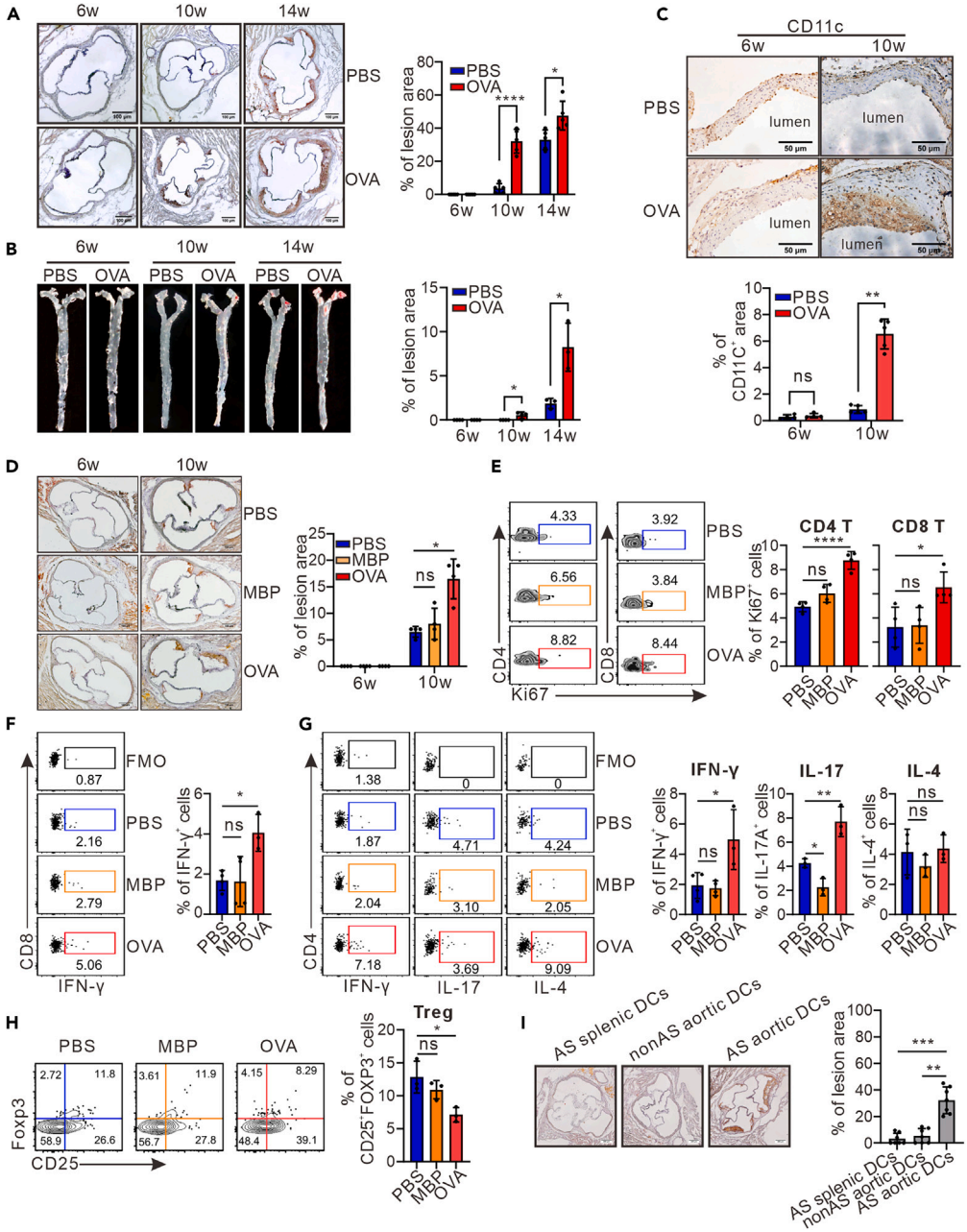

Figure 6. Pathogenic aortic DCs induce early onset of atherosclerotic plaques and atherosclerosis-like vascular inflammation in pre-atherosclerotic mice

Apoe$^{-/-}$ mice were immunized with OVA, MBP, or PBS on a continuously weekly basis after 6 weeks on a high-fat diet. Oil red staining was performed on cross-sections of aortic roots ($n = 5$)(scale bar: 100 μm) (A) or aorta *en face* (n = 3–4) (B) from the OVA- or PBS- immunized mice fed with a high-fat diet for different period of time as indicated. Immunohistochemical detection of CD11c expression was performed in paraffin sections of aortic roots (n = 4–5) (scale bar: 50 μm) (C). Oil red staining was performed on cross-sections of aortic roots from the OVA-, MBP- or PBS- immunized mice fed with a high-fat diet for 6 weeks and 10 weeks ($n = 4$) (scale bar: 100 μm) (D). Single cell suspensions from the aorta of mice with a high-fat diet for 10 weeks were prepared for FACS analysis. Plots and bar graphs showed the proportion of Ki67^{+}T cells in CD4^{+} T cells and CD8^{+}T cells ($n = 4$) (E); IFNγ expression in CD8^{+}T cells (n = 3–4) (F); IFNγ^{+}Th1, IL-17^{+}Th17, IL-4^{+}Th2 in CD4^{+}T cells (n = 3–4) (G); and CD25^{+}Foxp3^{+} Treg in CD4^{+} T cells ($n = 3$) (H). DCs sorted from the aorta or spleen were injected intravenously three consecutive times over a week into *Apoe*$^{-/-}$ mice receiving a high-fat diet for 6 weeks, and oil red staining was performed on frozen sections of aortic roots from recipient mice three weeks later ($n = 7$) (scale bar: 100 μm) (I). All data were shown as Mean ± SD, and analyzed using a two-tailed unpaired *t* test, two-tailed Mann-Whitney test, one-way ANOVA test, or Kruskal-Wallis test. *$p < 0.05$, **$p < 0.01$, ***$p < 0.001$, ****$p < 0.0001$. ns, no significant difference.

diseases. Firstly, we found that among APCs in three different atherosclerosis-related tissues regardless of before or after atherosclerosis, only DCs can present OVA antigen to stimulate T cells. Our data agree with and add to the results of mixed lymphocyte reactions *in vitro* mediated by DCs and Mϕ isolated from healthy mouse aorta.[23,24] Furthermore, within the DC lineage, we found that the onset of disease specifically enhanced the T cell stimulating capacity of aortic DCs, whereas that of splenic DCs was unaltered. Although the ability of DCs to present antigens in the aortic draining LNs of atherosclerotic mice was also slightly elevated, those DCs with a higher capacity to stimulate T cell activation were the migratory DCs (presumably aortic DCs that migrated to the draining LNs) rather than the resident DCs in the draining LNs. Finally, the identification of aortic DCs out of the three APCs in the above-mentioned tissues as major T cell stimulators during atherogenesis was further verified via cognate antigen *in vivo*, which was consistent with and improved the results of single cell suspensions from whole explanted intact atherosclerotic aorta without the separation of individual APCs.[37] Therefore, we have distinguished aortic DCs as the overwhelming presenters of disease-associated antigen under the atherosclerotic conditions. Following local T cell activation, the second unique disease-associated change identified for the aortic DCs was their distinguishing feature in promoting proinflammatory Th1 differentiation by upregulating its polarizing cytokine IL-12, in response to the onset of atherosclerosis, whereas other aortic cells were little altered during the development of the disease.

Another important finding in the current study is that we further identify the atherogenic role of aortic DCs at the subset level. To the best of our knowledge, we were the first to simultaneously classify the aortic DCs into moDCs, cDC1s, cDC2s, and pDCs, the latter of which was not further characterized due to their extremescarcity in aortic tissues (0.1–0.5% of total aortic cells), and comprehensively analyze their division of labor in atherosclerosis. Interestingly, we found that moDCs were the major disease-increased subset among the DCs in the atherosclerotic aorta in response to the increased GM-CSF levels in local tissues, a result consistent with a previous finding in GM-CSF$^{-/-}$ mice crossed to hypercholesterolemic low-density lipoprotein receptor null mice, where 60% reduction of DCs was found in aortic lesion sections, although in that study, the subset of the DCs affected were not further investigated.[38] Previous studies on the association of the moDC subset with atherosclerosis have mostly focused on their innate functions such as phagocytosis of apoptotic cells and formation of foam cells in the plaque,[39,40] whereas in current study, moDCs in atherosclerotic aorta were identified to be the major subset of DCs responsible for the disease-induced production of IL-12 for the enhanced Th1 differentiation in plaques, which is concordant with the inflammatory nature of this DC subset. In addition, we further found that aortic cDC1s were key drivers of T cell activation in atherosclerosis, which agrees with the reduced T cell activation in *Apoe*$^{-/-}$ mice after systematic removal of cDC1s via *irf8* depletion.[29] In particular, we demonstrated that atherosclerosis increased the effector:naive CD8$^+$ T cell ratio in the aorta, and enhanced the capacity of aortic cDC1s to cross-present antigens, presumably promoting the CD8$^+$T cell responses in the aorta to aggravate the disease; this supports the aortic on-site T cell priming theory by local APCs.[34,37] This is also consistent with elevated gene expression of T cell receptor signaling and cytotoxic pathways in CD8$^+$ T cells from patients with coronary artery disease.[41] The division of labor between T cell activation and differentiation by aortic cDCs and moDCs respectively can act synergistically to promote local adaptive immunity in inflammatory aorta. For example, cDC1s could activate CD8$^+$T cells and induce CD4$^+$T cell proliferation (thus increasing their abundance) and moDCs could induce those CD4$^+$T cells to differentiate into Th1 effectors to secrete inflammatory cytokines.

Unfortunately, there has been no ideal animal model in which local aortic DCs are specifically deleted so far, let alone local subset-specific deletion. To prove the causal role of aortic DCs in atherogenesis, we repeatedly immunized the hyperlipidemic mice with either OVA protein that has been proven to be a DC-presented antigen to expand OVA specific T cells, or MBP protein that could not be presented by DCs in our system. Interestingly, only the OVA-immunization accelerated the early onset of atherosclerosis. It is unlikely that the repeated immunization of an inert antigen such as OVA could lead to a non-specific secondary effect on cardiovascular disease in general, because vaccination for flu,[42] or COVID[43,44] had no perverse association with the risk of the cardiovascular events in the human population in a dose-response manner. Finally, the direct pathogenic roles of aortic DCs in the diseased setting were validated by the successful induction of early onset of atherosclerotic plaques in the pre-atherosclerotic *Apoe*$^{-/-}$ mouse under high-fat diet by aortic DCs, not splenic DCs from atherosclerotic mice, presumably presenting atherogenic native antigen(s) in the diseased vascular environment, which were absent in the healthy *Apoe*$^{+/+}$ mouse aorta.

Although lipid metabolic disorders and innate immune responses are heavily involved, the current study demonstrated that the development of atherosclerosis is strongly associated with antigen specific adaptive T cell immunity, mediated by local aortic DCs. Our precise identification of the immunopathological mechanisms at both tissue and cellular levels could be translated to the targeted intervention of disease progression with more accuracy and fewer complications. For example, intravascular injection of blocking antibodies for DC subset markers such as XCR1 or its ligand might mitigate the adaptive plaque injury. Further study is required to identify the tissue specific factors, such as local cognate antigen(s), cytokines, or growth factors that cause the atherogenic role of aortic DCs in the diseased vasculatures so that the restoration of these abnormal factors could lead to the early prevention of vascular inflammation before the pathogenic immune disorders occur.

Limitations of study

Further study is required to identify the tissue specific factors, such as regional metabolites, cytokines, growth factors, or even physical structures that cause the atherogenic role of aortic DCs in the diseased vasculatures so that the restoration of these abnormal factors could lead to the early prevention of vascular inflammation before the immune disorder occurs.

RESOURCE AVAILABILITY

Lead contact

Further information and requests for resources and reagents should be directed to and will be fulfilled by the lead contact, Yuekang Xu (yuekang.xu@hotmail.com).

Materials availability statement

This study did not generate new unique reagents.

Data and code availability

- All data reported in this article will be shared by the lead contact upon request.
- This article does not report the original code.
- Any additional information required to reanalyze the data reported in this article is available from the lead contact upon request.

ACKNOWLEDGMENTS

This work was supported by the National Natural Science Foundation of China Major Research Plan Project (91742101); Anhui International Science and Technology Collaborative Project, China (1604b0602017); Natural Science Foundation of Anhui Province, China (1608085MH160), and National Health and Medical Research Council grants, Australia (1143976, 1150425); Fund from Outstanding Innovative Research Team for Molecular Enzymology and Detection in Anhui Provincial Universities (2022AH010012) and Fund from Key Laboratory of Biomedicine in Gene Diseases and Health of Anhui Higher Education Institutes. All other authors have reported that they have no relationships relevant to the contents of this article to disclose.

AUTHOR CONTRIBUTIONS

W.Z. performed the experiments and analyzed the data; Z.C., D.M., M.L., J.W., and L.S. helped perform the experiments; A.M.L. edited the article; Y.X. conceived the ideas, designed the experiments, analyzed the data, and wrote the article. All authors have made a substantial, direct, and intellectual contribution to the work, and approved it for publication.

DECLARATION OF INTERESTS

The authors declare no competing interests.

STAR★METHODS

Detailed methods are provided in the online version of this paper and include the following:

- KEY RESOURCES TABLE
- EXPERIMENTAL MODEL AND STUDY PARTICIPANT DETAILS
- METHOD DETAILS
  - Adoptive transfer of DCs
  - Single cell suspensions and flow cytometry
  - Intracellular cytokine staining
  - RNA extraction and RT-qPCR analysis
  - *In vivo* cytotoxicity assay
  - Cognate antigen-specific T cell activation
  - OVA specific T cell proliferation
  - Histopathology
  - Cytokine assay
- QUANTIFICATION AND STATISTICAL ANALYSIS

SUPPLEMENTAL INFORMATION

Supplemental information can be found online at https://doi.org/10.1016/j.isci.2024.111144.

Received: April 4, 2024
Revised: September 3, 2024
Accepted: October 7, 2024
Published: October 10, 2024

REFERENCES

1. Doran, A.C. (2022). Inflammation Resolution: Implications for Atherosclerosis. Circ. Res. *130*, 130–148. https://doi.org/10.1161/CIRCRESAHA.121.319822.
2. Björkegren, J.L.M., and Lusis, A.J. (2022). Atherosclerosis: Recent developments. Cell *185*, 1630–1645. https://doi.org/10.1016/j.cell.2022.04.004.
3. Roy, P., Orecchioni, M., and Ley, K. (2022). How the immune system shapes atherosclerosis: roles of innate and adaptive immunity. Nat. Rev. Immunol. *22*, 251–265. https://doi.org/10.1038/s41577-021-00584-1.
4. Saigusa, R., Winkels, H., and Ley, K. (2020). T cell subsets and functions in atherosclerosis. Nat. Rev. Cardiol. *17*, 387–401. https://doi.org/10.1038/s41569-020-0352-5.
5. Fernandez, D.M., Rahman, A.H., Fernandez, N.F., Chudnovskiy, A., Amir, E.A.D., Amadori, L., Khan, N.S., Wong, C.K., Shamailova, R., Hill, C.A., et al. (2019). Single-cell immune landscape of human atherosclerotic plaques. Nat. Med. *25*, 1576–1588. https://doi.org/10.1038/s41591-019-0590-4.
6. Grivel, J.C., Ivanova, O., Pinegina, N., Blank, P.S., Shpektor, A., Margolis, L.B., and Vasilieva, E. (2011). Activation of T lymphocytes in atherosclerotic plaques. Arterioscler. Thromb. Vasc. Biol.

31, 2929–2937. https://doi.org/10.1161/ATVBAHA.111.237081.

7. Niwa, T., Wada, H., Ohashi, H., Iwamoto, N., Ohta, H., Kirii, H., Fujii, H., Saito, K., and Seishima, M. (2004). Interferon-gamma produced by bone marrow-derived cells attenuates atherosclerotic lesion formation in LDLR-deficient mice. J. Atherosclerosis Thromb. *11*, 79–87. https://doi.org/10.5551/jat.11.79.
8. Buono, C., Binder, C.J., Stavrakis, G., Witztum, J.L., Glimcher, L.H., and Lichtman, A.H. (2005). T-bet deficiency reduces atherosclerosis and alters plaque antigen-specific immune responses. Proc. Natl. Acad. Sci. USA *102*, 1596–1601. https://doi.org/10.1073/pnas.0409015102.
9. Hauer, A.D., Uyttenhove, C., de Vos, P., Stroobant, V., Renauld, J.C., van Berkel, T.J.C., van Snick, J., and Kuiper, J. (2005). Blockade of interleukin-12 function by protein vaccination attenuates atherosclerosis. Circulation *112*, 1054–1062. https://doi.org/10.1161/CIRCULATIONAHA.104.533463.
10. Wang, Q., Wang, Y., and Xu, D. (2022). Research progress on Th17 and T regulatory cells and their cytokines in regulating atherosclerosis. Front. Cardiovasc. Med. *9*, 929078. https://doi.org/10.3389/fcvm.2022.929078.
11. Gotsman, I., Grabie, N., Gupta, R., Dacosta, R., MacConmara, M., Lederer, J., Sukhova, G., Witztum, J.L., Sharpe, A.H., and Lichtman, A.H. (2006). Impaired regulatory T-cell response and enhanced atherosclerosis in the absence of inducible costimulatory molecule. Circulation *114*, 2047–2055.
12. Smith, E., Prasad, K.M.R., Butcher, M., Dobrian, A., Kolls, J.K., Ley, K., and Galkina, E. (2010). Blockade of interleukin-17A results in reduced atherosclerosis in apolipoprotein E-deficient mice. Circulation *121*, 1746–1755. https://doi.org/10.1161/CIRCULATIONAHA.109.924886.
13. Danzaki, K., Matsui, Y., Ikesue, M., Ohta, D., Ito, K., Kanayama, M., Kurotaki, D., Morimoto, J., Iwakura, Y., Yagita, H., et al. (2012). Interleukin-17A deficiency accelerates unstable atherosclerotic plaque formation in apolipoprotein E-deficient mice. Arterioscler. Thromb. Vasc. Biol. *32*, 273–280. https://doi.org/10.1161/ATVBAHA.111.229997.
14. King, V.L., Szilvassy, S.J., and Daugherty, A. (2002). Interleukin-4 deficiency decreases atherosclerotic lesion formation in a site-specific manner in female LDL receptor-/- mice. Arterioscler. Thromb. Vasc. Biol. *22*, 456–461. https://doi.org/10.1161/hq0302.104905.
15. Davenport, P., and Tipping, P.G. (2003). The role of interleukin-4 and interleukin-12 in the progression of atherosclerosis in apolipoprotein E-deficient mice. Am. J. Pathol. *163*, 1117–1125. https://doi.org/10.1016/S0002-9440(10)63471-2.
16. King, V.L., Cassis, L.A., and Daugherty, A. (2007). Interleukin-4 does not influence development of hypercholesterolemia or angiotensin II-induced atherosclerotic lesions in mice. Am. J. Pathol. *171*, 2040–2047. https://doi.org/10.2353/ajpath.2007.060857.
17. Schafer, S., and Zernecke, A. (2020). CD8(+) T Cells in Atherosclerosis. Cells *10*, 37. https://doi.org/10.3390/cells10010037.
18. Zernecke, A. (2015). Dendritic cells in atherosclerosis: evidence in mice and humans. Arterioscler. Thromb. Vasc. Biol. *35*, 763–770. https://doi.org/10.1161/ATVBAHA.114.303566.
19. Paulson, K.E., Zhu, S.N., Chen, M., Nurmohamed, S., Jongstra-Bilen, J., and Cybulsky, M.I. (2010). Resident intimal dendritic cells accumulate lipid and contribute to the initiation of atherosclerosis. Circ. Res. *106*, 383–390. https://doi.org/10.1161/CIRCRESAHA.109.210781.
20. Lacy, M., Bürger, C., Shami, A., Ahmadsei, M., Winkels, H., Nitz, K., van Tiel, C.M., Seijkens, T.T.P., Kusters, P.J.H., Karshovka, E., et al. (2021). Cell-specific and divergent roles of the CD40L-CD40 axis in atherosclerotic vascular disease. Nat. Commun. *12*, 3754. https://doi.org/10.1038/s41467-021-23909-z.
21. Rahman, M., Steuer, J., Gillgren, P., Végvári, Á., Liu, A., and Frostegård, J. (2019). Malondialdehyde Conjugated With Albumin Induces Pro-Inflammatory Activation of T Cells Isolated From Human Atherosclerotic Plaques Both Directly and Via Dendritic Cell-Mediated Mechanism. JACC. Basic Transl. Sci. *4*, 480–494. https://doi.org/10.1016/j.jacbts.2019.03.009.
22. Wang, F., Liu, M., Ma, D., Cai, Z., Liu, L., Wang, J., Zhang, W., Zhao, L., Zhai, C., and Xu, Y. (2023). Dendritic cell-expressed IDO alleviates atherosclerosis by expanding CD4+CD25+Foxp3+Tregs through IDO-Kyn-AHR axis. Int. Immunopharm. *116*, 109758. https://doi.org/10.1016/j.intimp.2023.109758.
23. Choi, J.H., Do, Y., Cheong, C., Koh, H., Boscardin, S.B., Oh, Y.S., Bozzacco, L., Trumpfheller, C., Park, C.G., and Steinman, R.M. (2009). Identification of antigen-presenting dendritic cells in mouse aorta and cardiac valves. J. Exp. Med. *206*, 497–505. https://doi.org/10.1084/jem.20082129.
24. Choi, J.H., Cheong, C., Dandamudi, D.B., Park, C.G., Rodriguez, A., Mehandru, S., Velinzon, K., Jung, I.H., Yoo, J.Y., Oh, G.T., and Steinman, R.M. (2011). Flt3 signaling-dependent dendritic cells protect against atherosclerosis. Immunity *35*, 819–831. https://doi.org/10.1016/j.immuni.2011.09.014.
25. Vallejo, J., Cochain, C., Zernecke, A., and Ley, K. (2021). Heterogeneity of immune cells in human atherosclerosis revealed by scRNA-Seq. Cardiovasc. Res. *117*, 2537–2543. https://doi.org/10.1093/cvr/cvab260.
26. Zernecke, A., Erhard, F., Weinberger, T., Schulz, C., Ley, K., Saliba, A.E., and Cochain, C. (2023). Integrated single-cell analysis based classification of vascular mononuclear phagocytes in mouse and human atherosclerosis. Cardiovasc. Res. *119*, 1676–1689. https://doi.org/10.1093/cvr/cvac161.
27. Sun, L., Zhang, W., Zhao, L., Zhao, Y., Wang, F., Lew, A.M., and Xu, Y. (2022). Self-Tolerance of Vascular Tissues Is Broken Down by Vascular Dendritic Cells in Response to Systemic Inflammation to Initiate Regional Autoinflammation. Front. Immunol. *13*, 823853. https://doi.org/10.3389/fimmu.2022.823853.
28. Gil-Pulido, J., Cochain, C., Lippert, M.A., Schneider, N., Butt, E., Amézaga, N., and Zernecke, A. (2017). Deletion of Batf3-dependent antigen-presenting cells does not affect atherosclerotic lesion formation in mice. PLoS One *12*, e0181947. https://doi.org/10.1371/journal.pone.0181947.
29. Clément, M., Haddad, Y., Raffort, J., Lareyre, F., Newland, S.A., Master, L., Harrison, J., Ozsvar-Kozma, M., Bruneval, P., Binder, C.J., et al. (2018). Deletion of IRF8 (Interferon Regulatory Factor 8)-Dependent Dendritic Cells Abrogates Proatherogenic Adaptive Immunity. Circ. Res. *122*, 813–820. https://doi.org/10.1161/CIRCRESAHA.118.312713.
30. Yu, Y.R.A., O'Koren, E.G., Hotten, D.F., Kan, M.J., Kopin, D., Nelson, E.R., Que, L., and Gunn, M.D. (2016). A Protocol for the Comprehensive Flow Cytometric Analysis of Immune Cells in Normal and Inflamed Murine Non-Lymphoid Tissues. PLoS One *11*, e0150606. https://doi.org/10.1371/journal.pone.0150606.
31. Langlet, C., Tamoutounour, S., Henri, S., Luche, H., Ardouin, L., Grégoire, C., Malissen, B., and Guilliams, M. (2012). CD64 expression distinguishes monocyte-derived and conventional dendritic cells and reveals their distinct role during intramuscular immunization. J. Immunol. *188*, 1751–1760. https://doi.org/10.4049/jimmunol.1102744.
32. Vidanapathirana, A.K., Goyne, J.M., Williamson, A.E., Pullen, B.J., Chhay, P., Sandeman, L., Bensalem, J., Sargeant, T.J., Grose, R., Crabtree, M.J., et al. (2022). Biological Sensing of Nitric Oxide in Macrophages and Atherosclerosis Using a Ruthenium-Based Sensor. Biomedicines *10*, 1807. https://doi.org/10.3390/biomedicines10081807.
33. Deczkowska, A., David, E., Ramadori, P., Pfister, D., Safran, M., Li, B., Giladi, A., Jaitin, D.A., Barboy, O., Cohen, M., et al. (2021). XCR1+ type 1 conventional dendritic cells drive liver pathology in non-alcoholic steatohepatitis. Nat. Med. *27*, 1043–1054. https://doi.org/10.1038/s41591-021-01344-3.
34. MacRitchie, N., Grassia, G., Noonan, J., Cole, J.E., Hughes, C.E., Schroeder, J., Benson, R.A., Cochain, C., Zernecke, A., Guzik, T.J., et al. (2020). The aorta can act as a site of naive CD4+ T-cell priming. Cardiovasc. Res. *116*, 306–316. https://doi.org/10.1093/cvr/cvz102.
35. Wolf, D., and Ley, K. (2019). Immunity and Inflammation in Atherosclerosis. Circ. Res. *124*, 315–327. https://doi.org/10.1161/CIRCRESAHA.118.313591.
36. Maganto-García, E., Tarrio, M.L., Grabie, N., Bu, D.X., and Lichtman, A.H. (2011). Dynamic changes in regulatory T cells are linked to levels of diet-induced hypercholesterolemia. Circulation *124*, 185–195. https://doi.org/10.1161/CIRCULATIONAHA.110.006411.
37. Koltsova, E.K., Garcia, Z., Chodaczek, G., Landau, M., McArdle, S., Scott, S.R., von Vietinghoff, S., Galkina, E., Miller, Y.I., Acton, S.T., and Ley, K. (2012). Dynamic T cell-APC interactions sustain chronic inflammation in atherosclerosis. J. Clin. Invest. *122*, 3114–3126. https://doi.org/10.1172/JCI61758.
38. Shaposhnik, Z., Wang, X., Weinstein, M., Bennett, B.J., and Lusis, A.J. (2007). Granulocyte macrophage colony-stimulating factor regulates dendritic cell content of atherosclerotic lesions. Arterioscler. Thromb. Vasc. Biol. *27*, 621–627.
39. Haka, A.S., Singh, R.K., Grosheva, I., Hoffner, H., Capetillo-Zarate, E., Chin, H.F., Anandasabapathy, N., and Maxfield, F.R. (2015). Monocyte-Derived Dendritic Cells Upregulate Extracellular Catabolism of Aggregated Low-Density Lipoprotein on Maturation, Leading to Foam Cell Formation. Arterioscler. Thromb. Vasc. Biol. *35*, 2092–2103. https://doi.org/10.1161/ATVBAHA.115.305843.
40. Dopheide, J.F., Sester, U., Schlitt, A., Horstick, G., Rupprecht, H.J., Münzel, T., and Blankenberg, S. (2007). Monocyte-derived

dendritic cells of patients with coronary artery disease show an increased expression of costimulatory molecules CD40, CD80 and CD86 in vitro. Coron. Artery Dis. *18*, 523–531. https://doi.org/10.1097/MCA.0b013e3282eff1ad.

41. Iqneibi, S., Saigusa, R., Khan, A., Oliaeimotlagh, M., Armstrong Suthahar, S.S., Kumar, S., Alimadadi, A., Durant, C.P., Ghosheh, Y., McNamara, C.A., et al. (2023). Single cell transcriptomics reveals recent CD8T cell receptor signaling in patients with coronary artery disease. Front. Immunol. *14*, 1239148. https://doi.org/10.3389/fimmu.2023.1239148.
42. Bhugra, P., Grandhi, G.R., Mszar, R., Satish, P., Singh, R., Blaha, M., Blankstein, R., Virani, S.S., Cainzos-Achirica, M., and Nasir, K. (2021). Determinants of Influenza Vaccine Uptake in Patients With Cardiovascular Disease and Strategies for Improvement. J. Am. Heart Assoc. *10*, e019671. https://doi.org/10.1161/JAHA.120.019671.
43. Song, J., Choi, S., Jeong, S., Chang, J.Y., Park, S.J., Oh, Y.H., Kim, J.S., Cho, Y., Byeon, K., Choi, J.Y., et al. (2024). Protective effect of vaccination on the risk of cardiovascular disease after SARS-CoV-2 infection. Clin. Res. Cardiol. *113*, 235–245. https://doi.org/10.1007/s00392-023-02271-8.
44. Wan, E.Y.F., Mok, A.H.Y., Yan, V.K.C., Chan, C.I.Y., Wang, B., Lai, F.T.T., Chui, C.S.L., Li, X., Wong, C.K.H., Yiu, K.H., et al. (2023). Association between BNT162b2 and CoronaVac vaccination and risk of CVD and mortality after COVID-19 infection: A population-based cohort study. Cell Rep. Med. *4*, 101195. https://doi.org/10.1016/j.xcrm.2023.101195.

STAR★METHODS

KEY RESOURCES TABLE

REAGENT or RESOURCE	SOURCE	IDENTIFIER
Antibodies		
FITC anti-mouse Ly-6G (Clone:1A8)	BioLegend	Cat#127605; RRID: AB_1236488
FITC anti-mouse/human CD45R/B220 (Clone: RA3-6B2)	Biolegend	Cat#103206; RRID: AB_312991
FITC anti-mouse CD19 (Clone: 1D3/CD19)	Biolegend	Cat#152404; RRID: AB_2629813
FITC anti-mouse CD8a (Clone: 53–6.7)	Biolegend	Cat#100706; RRID: AB_312745
FITC anti-Mouse I-A/I-E (Clone: 2G9)	BD Bioscience	Cat#553623; RRID:AB_394958
FITC anti-mouse MERTK (2B10C42)	Biolegend	Cat#151503; RRID: AB_2617034
PE anti-mouse CD11c (Clone: N418)	eBioscience	Cat#12-0114-82; RRID: AB_465552
PE anti-mouse CD11b (Clone: M1/70)	eBioscience	Cat#12-0112-82; RRID: AB_2734869
PE anti-mouse CD4-PE (Clone: GK1.5)	eBioscience	Cat#12-0041-82; RRID: AB_465506
PE anti-mouse Ly-6G (Clone: 1A8)	BioLegend	Cat#127607; RRID: AB_1186104
PE anti-mouse CD40 (Clone: FGK45)	Biolegend	Cat#157506; RRID: AB_2860731
PE anti-mouse CD64 (Clone: X54-5/7.1)	BioLegend	Cat#139304; RRID: AB_10612740
PE/Cy7 anti-mouse CD11c (Clone: N418)	Biolegend	Cat#117318; RRID: AB_493568
PE/Cy7 anti-mouse CD45 (Clone: 30-F11)	BD Bioscience	Cat#552848; RRID: AB_394489
PE/Cy7 anti-mouse CD3e (Clone: 145-2C11)	eBioscience	Cat#25-0031-82; RRID: AB_469572
PE/Cy7 anti-mouse F4/80 (Clone: BM8)	eBioscience	Cat#25-4801-82; RRID: AB_469653
PE/Cy7 anti-mouse MerTK (Clone: 2B10C42)	Biolegend	Cat#151521; RRID: AB_2876508
APC anti-mouse MHC-II (Clone: M5/114.15.2)	eBioscience	Cat#17-5321-82; RRID: AB_469455
APC anti-mouse CD19 (Clone: 6D5)	Biolegend	Cat#115512; RRID: AB_313647
APC anti-mouse CD25 (Clone: PC61.5)	eBioscience	Cat#17-0251-82; RRID: AB_469366
APC anti-mouse CD69 (Clone: H1.2F3)	eBioscience	Cat#17-0691-82; RRID: AB_1210795
APC anti-mouse SIINFEKL/H-2Kb (Clone: eBio25-D1.16 (25-D1.16))	eBioscience	Cat#17-5743-82; RRID: AB_1311286
APC anti- mouse CD8a (Clone: 53–6.7)	Biolegend	Cat#100712; RRID: AB_312751
APC anti- mouse CD64 (Clone: X54-5/7.1)	BioLegend	Cat#139306; RRID: AB_11219391
APC/Cy7 anti-mouse CD45 (Clone: 30-F11)	Biolegend	Cat#103116; RRID: AB_312981
BV785 anti-mouse CD62L (Clone: MEL-14)	BioLegend	Cat#104440; RRID: AB_2629685
BV785 anti-mouse/rat XCR1 (Clone: ZET)	BioLegend	Cat#148225; RRID: AB_2783119
BV421 anti-mouse CD11b (Clone: M1/70)	BioLegend	Cat#101251; RRID: AB_2562904
BV510 anti-mouse MHCII (Clone: 145-2C11)	BioLegend	Cat#100353; RRID: AB_2565879
BV510 anti-mouse CD3 (Clone: M5/114.15.2)	BioLegend	Cat#107636; RRID: AB_2734168
BV510 anti-mouse/human CD44 (Clone: IM7)	BioLegend	Cat#103044; RRID: AB_2650923
PerCP/Cy5.5 anti-mouse/rat XCR1 (Clone: ZET)	BioLegend	Cat#148207; RRID: AB_2564363
Alexa Fluor® 647 anti-mouse IL-17A (Clone: TC11-18H10)	BD Bioscience	Cat#560184; RRID: AB_1645204
APC anti-mouse IFN-γ (Clone: XMG1.2)	BD Bioscience	Cat#554413; RRID: AB_398551
APC anti-mouse IL-6 (Clone: MP5-20F3)	BD Bioscience	Cat#561367; RRID: AB_10679354
APC anti-mouse IL-12/IL-23 p40 (Clone: C15.6)	Biolegend	Cat#505206; RRID: AB_315370
APC anti-mouse IL-10 (Clone: JES5-16E3)	BD Bioscience	Cat#554468; RRID: AB_398558
APC anti-mouse IL-4 (Clone: 11B11)	BD Bioscience	Cat#554436; RRID: AB_398556
FITC anti-mouse/human Ki-67 (Clone: 11F6)	Biolegend	Cat#151212; RRID: AB_2814055

(*Continued on next page*)

Continued

REAGENT or RESOURCE	SOURCE	IDENTIFIER
Alexa Fluor 488 anti-mouse Foxp3 (Clone: MF23)	BD Bioscience	Cat#560403; RRID: AB_1645192
Anti-Mouse CD16/CD32 (Clone: 2.4G2)	BD Bioscience	Cat#553142; RRID: AB_394656
Experimental models: Cell lines		
Mouse B16 melanoma cells	Prof. Yongjun Dong from Tsinghua University, China	N/A
B16 melanoma cells expressing GM-CSF	Prof. Yongjun Dong from Tsinghua University, China	N/A
Experimental models: Organisms/strains		
C57BL/6 mice	Jiansu Qinglongshan Biotechnology Co., Ltd	Cat#SN525558705741893
Apoe$^{-/-}$ mice	Gempharmatech Co., Ltd	Strain NO. T001458
OT-II mice	Provided by Prof. Zhexiong Lian, University of Science and Technology of China	N/A
Software and algorithms		
ImageJ software	Wayne Rasband, NIH	N/A
Prism 8	GraphPad	N/A

EXPERIMENTAL MODEL AND STUDY PARTICIPANT DETAILS

Specific pathogen-free Apoe+/+ mice, Apoe−/− mice, and OT-II mice were (all are on C57BL/6 background) were housed in a specific pathogen-free environment in the Anhui Normal University Animal Facilities. For high-fat diet studies, 6-week-old Apoe+/+ mice and Apoe−/− mice were placed on a high-fat diet (21% fat, 0.15% cholesterol) over a period of 13 weeks to induce early-intermediate stage lesions in Apoe−/− mice (The detailed animal study design is shown in Table S1). Atherosclerotic lesions were quantified in the aortic root using oil red O staining. *En face* preparations of the aorta were used to determine the extents of lipid deposition. All procedures conducted on mice were in accordance with the conditions approved by the Institutional Animal Care and Use Committee of Anhui Normal University approval number (AHNU-ET2022015). B16 melanoma cells used were within 50 generations and incubated at 37°C with 5% CO2. All cell lines are tested negative for mycoplasma.

METHOD DETAILS

Adoptive transfer of DCs

0.1 × 106 DCs purified by FACS sorting were intravenously injected into Apoe−/− mice that had been on a high-fat diet for 6 weeks. The injections were administered consecutively three times within a week. Three weeks after the last injection, the mice were euthanized, and frozen sections of the aortic root were obtained for Oil Red O staining to assess the severity of atherosclerosis.

Single cell suspensions and flow cytometry

Aorta

Mice were anesthetized by injecting i.p. 500 μL of 5% chloral hydrate in PBS, and their vasculature was perfused by cardiac puncture with PBS containing 20 U/mL of heparin extensively to completely remove blood from all vessels, before single cell suspensions were prepared from aortic segments, including aortic sinus with valve or aortic arch and thoracic segments using previous methods22,27 with minor modifications. In brief, after full removal of the perivascular fat and cardiac muscle tissues, using micro-scissors under a dissecting microscope, single cell suspensions from 2 aortas were prepared by incubation with 2 mL enzyme mixture containing 400 U/mL collagenase I, 120 U/mL collagenase XI, 60 U/mL hyaluronidase, and 60 U/mL DNase1 in modified Dulbecco's PBS with calcium and magnesium for 60 min at 37°C with gentle shaking. A cell suspension was obtained by mashing the vascular tissues through a 70-μm strainer.

Spleen

Splenic single cell suspensions were prepared by treatment with 0.5 mg/mL of collagenase type II for 55 min and 2 mM of EDTA for another 5 min. Erythrocytes were then removed by exposure to red blood cell lysis buffer.

Draining lymph nodes (LN)

Single cell suspensions were prepared by taking mouse renal lymph nodes and grinding them through a 200 mesh cell sieve.

Single cell suspensions of aortic single cells and splenocytes were stained with indicated antibodies in the excess amounts of Fc receptor blocking antibody for 30 min on ice and added propidium iodide (1 mg/mL) at the final wash to stain dead cells. Flow cytometric analysis was performed with flow cytometer (FACS Melody, BD Biosciences, San Jose, CA, USA). Flow Jo software was used to analyze the data.

Intracellular cytokine staining

The aortic single cells and splenocytes were isolated and then stained with antibodies against CD45, CD11b, CD11c, F4/80, Ly6G, MHC-II, and NK1.1 or CD45, CD3, CD4, CD8 and CD11b (Major Resources Table). Then, cells were fixed, perforated and stained intracellularly with IL-12/IL-23 p40, IL-6, IFN-γ, IL-17A, IL-10 or IL-4 for 30 min on ice. Flow-cytometric analysis was performed with BD FACS Melody flow cytometer.

RNA extraction and RT-qPCR analysis

Trizol (Sangon Biotech, B511311) was used to extract total RNA at 42°C for 5 min, and genomic DNA was removed at 42°C for 15 min and reversely transcribed to cDNA at 95°C for 3 min with the PrimeScript RT kit (Accurate Biology, AG11705) following the manufacturer's instructions. The expression of *GM-CSF* and *β-actin* on mRNA level was quantified by CFX96 real-time PCR detection system (Bio-Rad), and the data was analyzed by CFX Manager Software. The primer sequences for the indicated genes are: *β-actin* forward: AGC CAT GTA CGT AGC CAT CC, *β-actin* reverse: TCC CTC TCA GCT GTG GTG GTG AA; *GM-CSF* forward: TCG TCT CTA ACG AGT TCT CCT T, *GM-CSF* reverse: CGT AGA CCC TGC TCG AAT ATC T. All the data were expressed relative to β-actin as reference genes.

In vivo cytotoxicity assay

Mice were immunized *i.p.* with OVA (500 μg) or irrelevant-peptide once per week for two consecutive weeks. Three days after last immunization, splenocytes from C57BL/6 mice were differentially labeled with high concentration of CFSE (10 μM) and loaded with OVA protein, or labeled with low concentration of CFSE (2 μM) but not loaded with OVA protein as $CFSE^{high}$ and $CSFE^{low}$ target cells respectively, before a total of 10×10^6 target cells per mouse were injected, consisting of a mixture of the $CFSE^{high}$ and $CSFE^{low}$ cells in 1:1 ratio. 24h later, the percentages of residual $CFSE^{high}$ and $CSFE^{low}$ target cells remaining in the recipients' spleens or aorta were analyzed by FACS. The percentage of specific lysis was calculated using following equation: % specific lysis = 100%–(%$CFSE^{high}$/%$CFSE^{low}$)/(%$CFSE^{high}$ in Ctrl/%$CFSE^{low}$ in Ctrl).

Cognate antigen-specific T cell activation

Draining lymph nodes of aorta from normal or atherosclerotic mice were removed and prepared into single cell suspensions. The $CD4^+CD44^-CD62L^+$ naive T cells and $CD4^+CD44^+CD62L^-$ T_{EM} cells were sorted by BD FACS Melody flow cytometry, which were then incubated with sorted DCs, Mϕ or B cells from aorta or spleen for 12 h in 96-well round bottom plate. 5000 T cells were co-culture with APCs at 1:10 ratio and IFNγ and TNFα in supernatant were detected by enzyme-linked immunosorbent assay.

OVA specific T cell proliferation

In vitro: FACS-sorted OT-II $CD4^+$ T cells were incubated with 5μM CFSE in 1 mL PBS per 1×10^7 cells for 10 min at 37°C. FACS-sorted B cells, Mϕ and DCs in spleens or aorta were co-cultured with the CFSE-labeled OT-II $CD4^+$T cells in 96-well round bottom plate at 1:10 ratio for 3 days in the presence of 200 μg/mL OVA before FACS analysis. Proliferation of OT-II $CD4^+$T cells was determined by flow cytometry using the CFSE dilution assay.

In vivo: FACS-sorted OT-II $CD4^+$T cells were incubated with 5μM CFSE in 1 mL PBS per 1×10^7 cells for 10 min at 37°C. 6×10^6 CFSE labeled cells in 100μL PBS were then *i.v.* injected into mice. After 24 h, mice were *i.v.* injected with OVA protein (100 μg) in 100 μL PBS. After 2 days, aortic single cells and splenocytes were isolated and stained with FACS antibodies against CD45 and CD4 for 30 min on ice. Proliferation of OT-II-derived $CD4^+$ T cells was determined by flow cytometry using the CFSE dilution assay.

Histopathology

100μL OVA (500 μg) or PBS were mixed with equal volume of complete Freund's Adjuvant (Sigma-Aldrich), emulsified by vibration and injected *i.p.* into $ApoE^{-/-}$ mice after 6 weeks high-fat diet. Then, OVA (500 μg) or PBS was injected subcutaneously in the back of these mice once a week. 4 or 8 weeks after first immunization the mice were sacrificed. The complete thoracoabdominal aorta including the aortic arch was removed, fixed with 4% paraformaldehyde for 2 h after complete removal of fat from the adventitia, and then stained with oil red O. The hearts were taken off, fixed in 4% paraformaldehyde for 2 h, and placed in a PBS sucrose 30% solution overnight at 4°C before being included in a cutting medium and frozen at −20°C. Successive 10-μm transversal sections of aortic sinus were obtained. The lipid on slices were assessed in aortic roots by staining for lipid depositions with oil red O. Oil red O staining on slices was observed under an Olympus microscope (Olympus BX61), and plaque area was quantified by ImageJ software with the area of the plaque as a proportion of the aortic wall area calculated.

Cytokine assay

Normal mice or atherosclerotic mice were injected *i.p.* with 300 mg Brefeldin A (Sigma-Aldrich) to block cytokine release and culled 5 h later. Briefly, aortas and spleens were harvested and stained for intracellular cytokines via FACS as detailed in Supplementary material.

QUANTIFICATION AND STATISTICAL ANALYSIS

Data were presented as mean ± SD and analyzed using Prism (Graph Pad Software). Normality tests were performed using Shapiro-Wilk test. Differences between 2 groups were compared using Unpaired *t* test or Mann Whitney test. Differences among 3 or more groups were compared using one-way ANOVA, followed by Holm-Šídák's multiple comparisons test or Kruskal-Wallis test, followed by Dunn's multiple comparisons test. The $p < 0.05$ was considered statistically significant.